

Machine learning for solar irradiance forecasting of photovoltaic system



Jiaming Li ^{a,*}, John K. Ward ^b, Jingnan Tong ^b, Lyle Collins ^b, Glenn Platt ^b

^a CSIRO CCI, Australia

^b CSIRO Energy Technology, Australia

ARTICLE INFO

Article history:

Received 7 September 2015
Received in revised form
24 November 2015
Accepted 31 December 2015
Available online 18 January 2016

Keywords:

Virtual power station
Renewable energy optimization
Genetic algorithm
Hidden Markov model
SVM regression
Neural networks

ABSTRACT

Photovoltaic generation of electricity is an important renewable energy source, and large numbers of relatively small photovoltaic systems are proliferating around the world. Today it is widely acknowledged by power producers, utility companies and independent system operators that it is only through advanced forecasting, communications and control that these distributed resources can collectively provide a firm, dispatchable generation capacity to the electricity market. One of the challenges of realizing such a goal is the precise forecasting of the output of individual photovoltaic systems, which is affected by a lot of factors. This paper introduces our short-term solar irradiance forecasting algorithms based on machine learning methodologies, Hidden Markov Model and SVM regression. A series of experimental evaluations are presented to analyze the relative performance of the techniques in order to show the importance of these methodologies. The Matlab interface, the Weather Forecasting Platform, has been used for these evaluations. The experiments are performed using the dataset generated by Australian Bureau of Meteorology. The experimental results show that our machine learning based forecasting algorithms can precisely predict future 5–30 min solar irradiance under different weather conditions.

© 2016 Elsevier Ltd. All rights reserved.

1. Introduction

The world has abundant solar energy resources. Photovoltaic (PV) technology has become one of several promising alternatives for use in energy technology [1]. Yet many critics of the widespread use of solar energy cite its intermittency, or the challenges around predicting the future output of a solar generator. The Virtual Power Station (VPS) [2–4] conducted by CSIRO aims to address such concerns by combining a large number of geographically disperse, and technically diverse, small scale renewable energy generators that will allow them to present to the electricity market as a single reliable dispatchable entity. The aggregated energy of the VPS can be sourced from a large number of small energy generation and storage systems, such as roof-mounted solar PV panels, and associated grid-connected battery systems installed in individual domestic houses. These individual systems are then aggregated together, to form a “virtual power station”, with one coordinated response, of benefit to the wider electricity network. However,

integration of large amounts of PV into the electricity grid poses technical challenges due to the fluctuating characteristics of available solar energy sources. PV output is not easily predictable in advance and varies based on both weather conditions and site-specific conditions. Such variability of solar energy resources at ground level thus raises concerns regarding how to manage and integrate output from the VPS to the power grid.

Given the issues above, there is increasing interest in more precise modeling and forecasting of solar power. Irradiance is a measurement of solar power and usually measures the power per unit area. Most researches consider the solar irradiance forecasting at a site, which is essentially the same problem as forecasting solar power. The ability to forecast solar irradiation will enable power grid operators to be able to ensure the quality and control of solar electricity supplies in an environment of greater solar panel usage, allow them to better accommodate highly variable electricity generation in their scheduling, dispatching, and regulation of power. In particular, the possibility to forecast solar irradiance can become fundamental in making power dispatch plans, and also a useful reference for improving the control algorithms of battery charge controllers. Ultimately, the development of more accurate

* Corresponding author.

E-mail address: jiaming.li@csiro.au (J. Li).

methods for modeling and forecasting solar irradiance remains a key requirement of our future energy system.

Different solar irradiance forecast methodologies have been proposed for various time horizons. Some of them forecast up to 24 h or even more [5]. Whilst useful for long-term forecasts, such techniques don't meet the demands of many electricity markets, for example the Australian electricity market uses 5-min dispatch price and a 30-min trading price. Thus, accurate short-term forecast are essential for energy market participation, both due to forward contracting and the need for a predictable, stable and smooth supply. Accurately forecasting direct normal irradiance or global horizontal irradiance in the seconds-to-minutes time-frame ultimately enables finely-tuned dynamic operational schedules that can reduce fuel costs, increase network stability or maximize system lifetimes.

Machine learning methods have been used to solve complicated practical problems in various areas [6–11] and are becoming more and more popular nowadays. Several machine learning based methodologies, such as genetic algorithm (GA) [12] and neural networks (NNs) [13,14], have been proposed and applied for modeling and forecasting of solar irradiance [15–22]. Quaiyum et al. [15] presented a neural networks and genetic algorithm model to predict the solar irradiance data from both endogenous and exogenous variables. Mellit et al. [16] developed a neural network-based genetic algorithm model for generating the sizing curve of stand-alone photovoltaic systems. Mellit et al. [17] developed a multilayer model to forecast the solar irradiance 24 h ahead. The inputs of proposed model use mean daily irradiance and mean daily air temperature and the output is solar irradiance data 24 h ahead. Mellit et al. [18] also developed radial basis function based neural network model for prediction solar radiation data. Kemmoku et al. [19] used a multistage neural network to predict irradiance of the next day. The input data to the network are the average atmospheric pressure, predicted by another neural network and various weather data of the previous day. Irradiance forecast by the multi-stage and the single-stage neural networks are compared with measured irradiance. Sfetos et al. [20] used neural network to make one-step predictions of hourly values of global irradiance and to compare them with linear time series models that work by predicting the clearness index. They introduced an approach for forecasting hourly solar irradiance using various neural network based techniques and also investigated other meteorological variables such as temperature, wind speed, and pressure. Mihalakakou et al. [21] developed a total solar irradiance time series simulation model based on neural network and applied it in Athens. The neural network was identified as the model with the least error. Hocaoglu et al. [22] incorporate multi-stage to time-delay neural network models for the prediction of hourly solar radiation. But the problems for these methods are as follows.

- Genetic algorithm (GA) [10] is an optimum search technique based on the concepts of natural selection and survival of the fittest, has been successfully applied to many difficult problems [9–11]. But for our solar irradiance forecasting issue, the first and one of the most difficult questions is the physical model definition, which describes the physical state and dynamic motion of the atmosphere defined by mathematical equations. Current GA based solar irradiance forecasting algorithms [15,16] couldn't give such physical properly.
- Neural Networks (NNs) are an information processing paradigm that is inspired by the way biological nervous systems, such as the brain, process information. The key element of this paradigm is the novel structure of the information processing system. It is composed of a large number of highly interconnected

processing elements (neurons) working in unison to solve specific problems. The same as GA, NN has been successfully applied in a lot areas [22,23]. But for our application it cannot easily be determined which variables are the most important contributors to future solar irradiance, what novel structure of the network is optimal, and a neural network model may contain a number of unimportant input variables that the developer fails to appreciate.

To avoid the problems of GA and NNs, this paper introduces our short-term solar forecasting algorithms using Hidden Markov Model and SVM regression based on the dataset gathered from the Australian Bureau of Meteorology (BOM). In order to evaluate the generalizability of the forecasting algorithms, the evaluations are performed under different weather conditions for forecasting future 5–30 min solar irradiance. The paper is organized as follows. Section 2 briefly presents our Matlab interface, the Weather Forecasting Platform, for evaluating our developed solar irradiance forecasting algorithms. Section 3 introduces the BOM dataset used for comparison. Section 4 introduces our solar forecasting algorithms in details. Section 5 provides a series of experimental results to evaluate solar irradiance forecasting performance. Finally, a conclusion is drawn in Section 6.

2. Solar irradiance forecasting platform

We developed a Matlab interface – the Weather Forecasting Platform (WFP), which is shown in Fig. 1. The WFP is designed so that historical and forecast data - data that is necessary to perform a forecast - can be delivered to the different forecasting algorithms (an example of which is a neural networks algorithm) in a consistent manner. Another primary purpose of the WFP, is to ensure the forecasting algorithms act in a causal manner, so algorithms don't accidentally 'cheat' by looking at future data (from the perspective of the WFP). The arrows in Fig. 1 represent the flow of the data – not simply communication between the modules, as communication between all of the connected modules is bidirectional.

The WFP is designed to work as follows:

1. The user application provides the WFP with a forecast request. The request includes such details as:
 - a. Which of the forecasting algorithms is to perform the forecast. Note that potentially all of the forecasting algorithms can be requested to perform the forecast, because of the common forecast output format from the WFP, makes a comparative analysis of the differing forecasting algorithms easy.
 - b. The weather parameter to be forecasted – e.g. irradiance, temperature. It is irradiance that is the focus of the remainder of the paper.
 - c. The present time. By 'present' it is meant the time for which the WFP can consider to be the current time, such that any request to get data from a future time is inhibited. This is necessary to enforce the real-world requirement that the forecasting algorithms be causal.
 - d. Any forecasting algorithm parameters of interest. Parameters such as frequency of the forecast data, forecast horizon, or any other configuration parameters are all valid parameters.
2. The WFP passes on the relevant data from the request to the one or many forecasting algorithms identified in (1a).
3. The algorithms then make independent decisions on what data is necessary for them to perform their requested forecasting task. The forecasting algorithms then respond to the forecast request by sending a data request to the WFP.

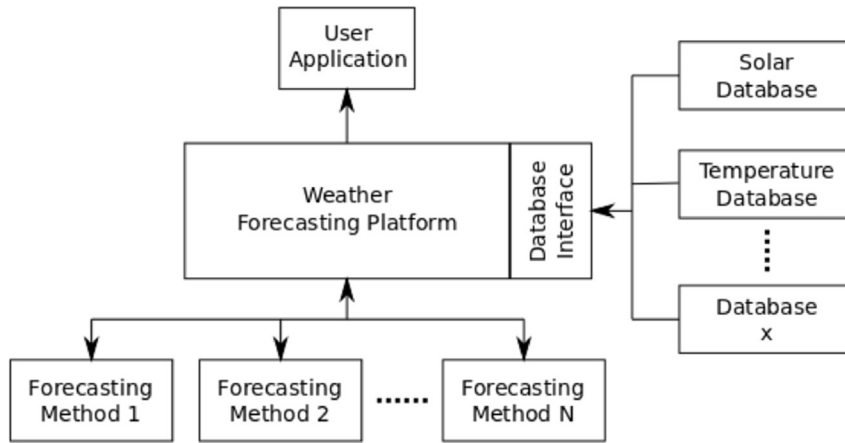


Fig. 1. Weather forecasting platform.

4. The WFP, after checking causality is not breached, sends the data request to the appropriate databases to gather as much data as possible in an attempt to fulfill the request in its entirety. The database interface layer (identified in Fig. 1) acts to ensure that all data received by the WFP is in a consistent format.
5. The WFP passes the data back to the forecasting algorithms. The forecasting algorithms now perform their respective forecasting tasks independently.
6. Once forecasting is complete, the forecast is sent to the WFP.
7. The WFP passes the forecast to the user application.

3. BOM data

Climate is the typical weather conditions experienced at any location or area. To better understand our climate, the Bureau of Meteorology (BOM) collects information from across Australia, including rainfall, wind, temperature, fog, thunder, humidity, pressure, ocean temperatures and sunshine data. BOM data is based on past weather and climate datasets provided online, which includes data from around 18,000 sites. The BOM provides free access to historical climate (weather) data from these sites. The daily weather observations for the previous 14 months of the area of interest can be downloaded. Two kinds of data are used in our algorithms, i.e. weather data and solar data. They are both sampled in 1 min. There are 44 parameters in weather data, covering temperature, humidity, atmospheric pressure, through to irradiance and the statistical qualities of these measured values.

Fig. 2 shows examples of BOM data for the days of 3rd and 4th of January 2012, weather data (top) and solar data (bottom). Fig. 3 is the examples of irradiance distribution data for different days. From the figures we can see that the data is not smooth. It varies with time because of weather and factors such as cloud changes.

4. Short-term solar irradiance forecasting algorithms based on BOM data

Short-term solar irradiance forecasting is to use sensor data both for solar and weather information from BOM database introduced in Section 3 to predict future 5–30 min irradiance.

4.1. Forecasting based on hidden Markov model

4.1.1. Hidden Markov model

Hidden Markov Models (HMMs) [24–26] are a good

methodology for time series analysis, modeling and prediction because the models can encode statistic relationships among variables of interest. These models are constructed via a learning process on some training data from past observations. The learnt models can then be used for forecasting.

Weather is time series information. HMMs are chosen to model the output of PV system because they can infer optimal hidden states from observation sensor data while other modeling technologies, such as genetic algorithm [12] and neural networks [22,23], can only model what will be observed from what has already been observed. Generally speaking, a HMM is a statistical model in which the system being modeled is assumed to be a Markov process with unknown parameters. A Markov process is a mathematical model for the random evolution of a memoryless system. That is, the likelihood of a given future state at any given moment depends only on its present state and not on any past states.

The most common HMM structure is a finite set of states, each of which is associated with a (generally multidimensional) probability distribution [27]. Transitions among the states are governed by a set of probabilities called transition probabilities. In any given state, there is some probability that an outcome or observation is generated, according to an associated probability distribution. It is only the outcome, not the state, that is visible to an external observer and therefore states are “hidden”.

To define a HMM, three basic components are needed:

A vector containing the prior probability of each hidden state: the initial state distribution, $\pi = \pi_i$, where $\pi_i = p\{q_0 = i\}$, for $1 \leq i \leq N$. Here N is the number of states of the model, and q_0 denotes the initial state.

A set of state transition probabilities $\Lambda = a_{ij}$. Define

$$a_{ij} = p\{q_{t+1} = j | q_t = i\}, \quad 1 \leq i, j \leq N, \quad (1)$$

where q_t denotes the current state. Transition probabilities should satisfy the normal stochastic constraints, $0 \leq a_{ij} \leq 1$ for $1 \leq i, j \leq N$, and $\sum a_{ij} = 1$ for $1 \leq i \leq N$, $1 \leq j \leq N$.

The probability of the observation given a state, $B = \{b_j(k)\}$. Define

$$b_j(k) = p\{O_t = v_k | q_t = j\}, \quad 1 \leq j \leq N, 1 \leq k \leq M, \quad (2)$$

where v_k denotes the k th observation, M the number of observation, and O_t the current parameter vector. The following stochastic constraints must be satisfied: $0 \leq b_j(k) \leq 1$ for $1 \leq j \leq N$, $1 \leq k \leq M$, and $\sum b_j(k) = 1$ for $1 \leq j \leq N$, $1 \leq k \leq M$.

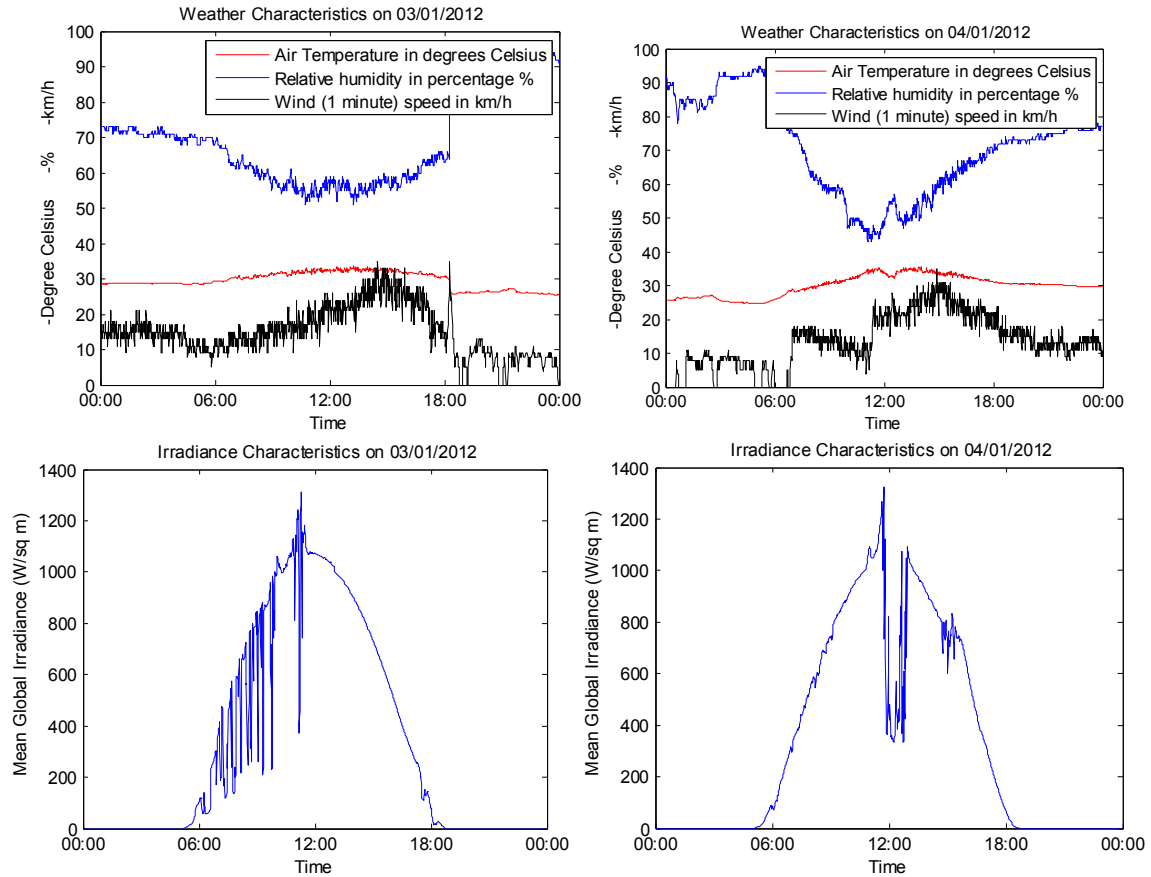


Fig. 2. Examples of BOM data.

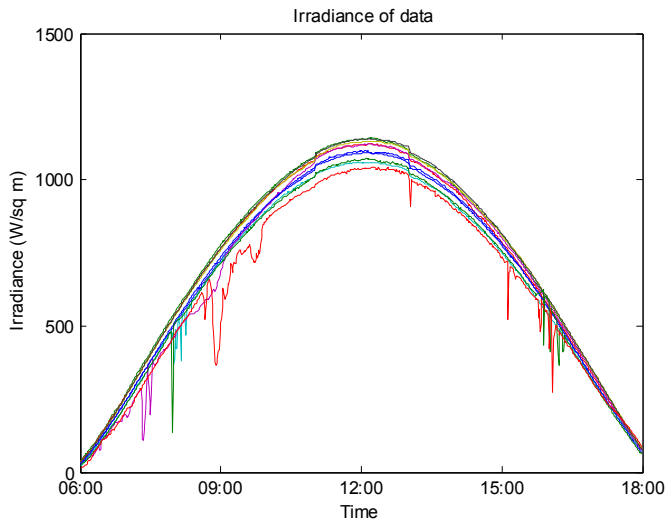


Fig. 3. Examples of irradiance data.

4.1.2. Hidden Markov model for solar irradiance forecasting

The main purpose of HMM is to develop a proper model to predict the precise future solar irradiance under variable climatic conditions. In modeling solar irradiance, transitions between the same or different hidden states can be forecasted using state transition matrix A and state-dependent observation matrices B . For forecasting, the state transition matrix A and state dependent

observation matrices B are based on measurement of the system. An irradiance forecasting process for a PV system can be easily implemented. The only pre-defined parameters of the HMM are the number of observation states and the number of hidden states. Generally speaking, the observation states are what can be measured. The hidden states may not have real-world/physical meaning, and are generally selected based on experience and/or experimentation. Fig. 4 shows an example of a HMM with five sensor readings as the observe states (above the dash line), and four hidden states (below the dash line). The arrows show the transition probabilities between hidden states. The training process is used to find the HMM parameters that maximize the probability $P(O|\pi, A, B)$. This process is performed using the recursive Baum-Welch algorithm as described in Ref. [27].

The future solar irradiance depends upon several factors, especially the meteorological conditions such as current and/or past solar irradiance, relative humidity, ambient temperature and wind speed. In our irradiance forecasting process, observation states include a) past, current and forecasted air temperature, b) past, current and forecasted relative humidity, c) past, current and forecasted wind speed d) past and current irradiance. The HMM calculates the likelihood of the new data's fitness to the learnt HMM. If the likelihood is high, the irradiance selected from possible range of irradiances is used for predicted irradiance. Fig. 5 is a schematic diagram of the idea, in which the blue line represents data weather forecasting; the black line represents past weather and irradiance data. The forecasting data is generated by past 30 min data.

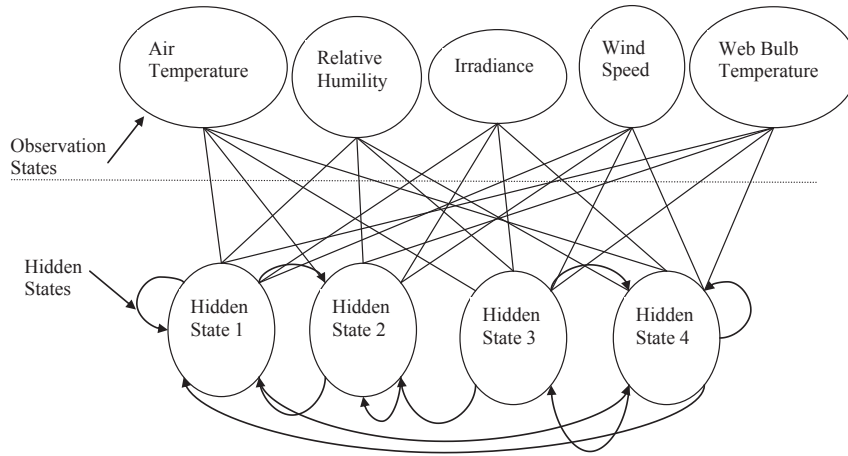


Fig. 4. An example of a HMM with five sensor readings as the observe states (above the dashed line), and four hidden states (below the dashed line). The arrows show the transition probabilities between hidden states.

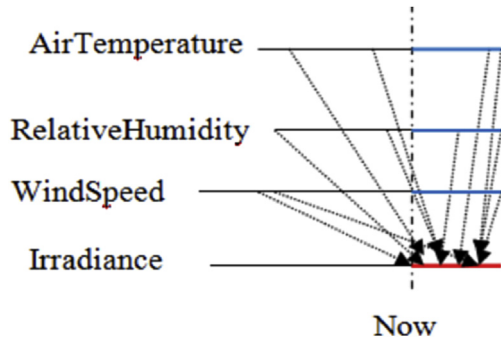


Fig. 5. Forecasting parameters.

4.2. Forecasting based on irradiance gradient regression using SVM

Solar irradiance changes during the day. Under the same cloud and weather conditions, this change follows a general pattern. At any time, there exists a proper irradiance gradient. If we know this gradient, we can forecast the irradiance in the future easily. This process is the irradiance gradient regression, which is implemented by SVM.

4.2.1. Support vector machine

The basic idea of SVM is to map the training data from the input space into a higher dimensional feature space (Fig. 6) via function Φ and then construct a separating hyperplane with maximum margin in the feature space. Given a training set of data $x_i \in R^n, i = 1, 2, \dots, l$, where l corresponds to the size of the training data and $y_i = \pm 1$ class labels, SVM will find a hyperplane direction W and an offset scalar b such that $f(x) = W \times \Phi(x) + b \geq 0$ for positive examples and $f(x) = W \times \Phi(x) + b \leq 0$ for negative examples. Consequently, although we cannot find a linear function in the input space to decide what type the given data is, we can easily find an optimal hyperplane that can clearly discriminate between the two types of data.

Consider a set of training data where each $x_i \in R^n$ denotes the input space of the sample and has a corresponding target value $y_i \in R$ for $i = 1, 2, \dots, l$, where l corresponds to the size of the training data. The idea of the regression problem is to determine a function that can approximate future values accurately.

The generic SVM regression (SVR) estimating function takes the form

$$f(x) = (w \cdot \Phi(x)) + b \tag{3}$$

where Φ denotes a nonlinear transformation from R^n to high-dimensional space. Our goal is to find the value of W and b

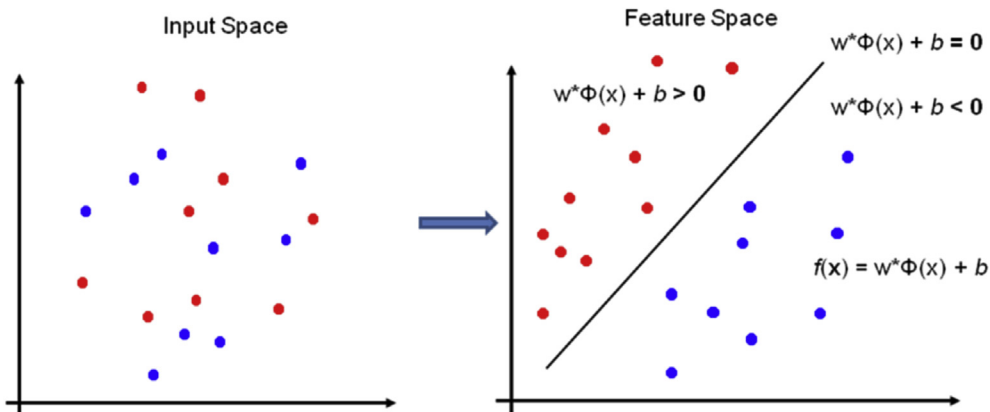


Fig. 6. SVM - solve the binary classification problem, separating red balls from blue balls. (For interpretation of the references to color in this figure legend, the reader is referred to the web version of this article.)

such that values of x can be determined by minimizing the regression risk

$$R_{reg}(f) = C \sum_{i=0}^l \Gamma(f(x_i) - y_i) + \frac{1}{2} \|W\|^2 \quad (4)$$

where Γ is a cost function, C is a constant, and vector w can be written in terms of data points as

$$w = \sum_{i=1}^l (\alpha_i - \alpha_i^*) \Phi(x_i) \quad (5)$$

By substituting Eq. (5) into Eq. (3), the generic equation can be rewritten as

$$f(x) = \sum_{i=1}^l (\alpha_i - \alpha_i^*) (\Phi(x_i) \cdot \Phi(x)) + b = \sum_{i=1}^l (\alpha_i - \alpha_i^*) k(x_i, x) + b \quad (6)$$

In Eq. (6), the dot product can be replaced with function $k(x_i, x)$, known as the kernel function. Kernel functions enable the dot product to be performed in high-dimensional feature space using low-dimensional space data input without knowing the transformation Φ . All kernel functions must satisfy Mercer's condition that corresponds to the inner product of some feature space. For nonlinear SVM, there are a number of kernel functions which have been found to provide good performance, such as polynomials and radial basis function (RBF). The RBF is commonly used as the kernel for regression

$$k(x, x_i) = \exp\left(-\frac{\|x - x_i\|^2}{2\sigma^2}\right) \quad (7)$$

The ϵ -insensitive loss function is the most widely used cost function (7). The function is in the form

$$\Gamma(f(x) - y) = \begin{cases} |f(x) - y| - \epsilon, & \text{for } |f(x) - y| \geq \epsilon \\ 0, & \text{otherwise} \end{cases} \quad (8)$$

By solving the quadratic optimization problem, the regression risk in Eq. (4) and the ϵ -insensitive loss function Eq. (8) can be minimized

$$\frac{1}{2} \sum_{i,j=1}^l (\alpha_i^* - \alpha_i) (\alpha_j^* - \alpha_j) k(x_i - x_j) - \sum_{i=1}^l \alpha_i^* (y_i - \epsilon) - \alpha_i (y_i + \epsilon)$$

subject to

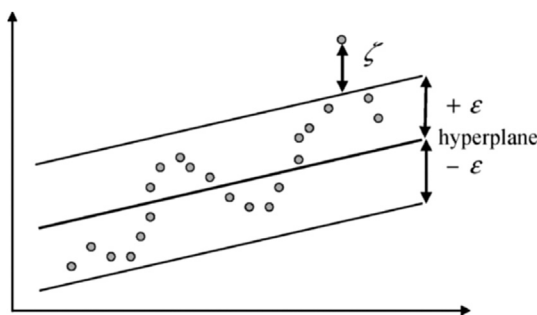


Fig. 7. SVM to fit a tube with radius ϵ to the data and positive slack variables ζ_i measuring the points lying outside of the tube.

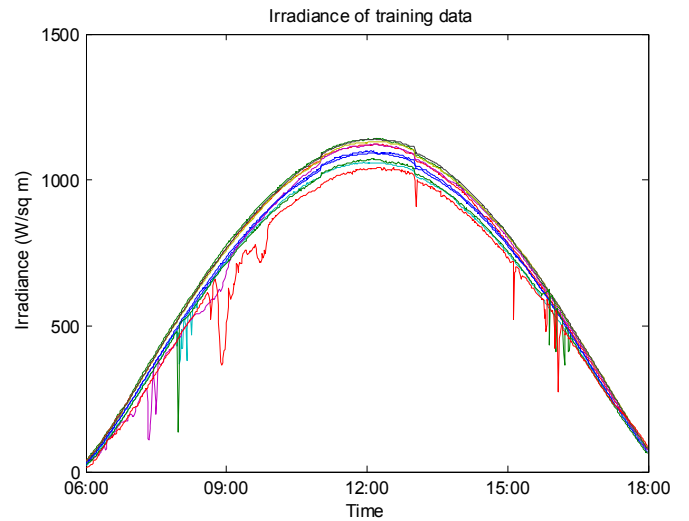


Fig. 8. Training data for Irradiance Gradient Regression.

$$\sum_{i=1}^l \alpha_i - \alpha_i^* = 0, \alpha_i, \alpha_i^* \in [0, C] \quad (9)$$

The Lagrange multipliers α_i and α_i^* represent solutions to the above quadratic problem, which act as forces pushing predictions toward target value y_i . Only the nonzero values of the Lagrange multipliers in Eq. (9) are useful in forecasting the regression line and are known as support vectors. For all points inside the ϵ tube, the Lagrange multipliers equal to zero do not contribute to the regression function. Only if the requirement $|f(x) - y| \geq \epsilon$ (see Fig. 7) is fulfilled, Lagrange multipliers may be nonzero values and used as support vectors.

Now, we have solved the value of w in terms of the Lagrange multipliers. For the variable b , it can be computed by applying the Karush–Kuhn–Tucker (KKT) conditions that, in this case, imply that the product of the Lagrange multipliers and constrains has to equal to 0.

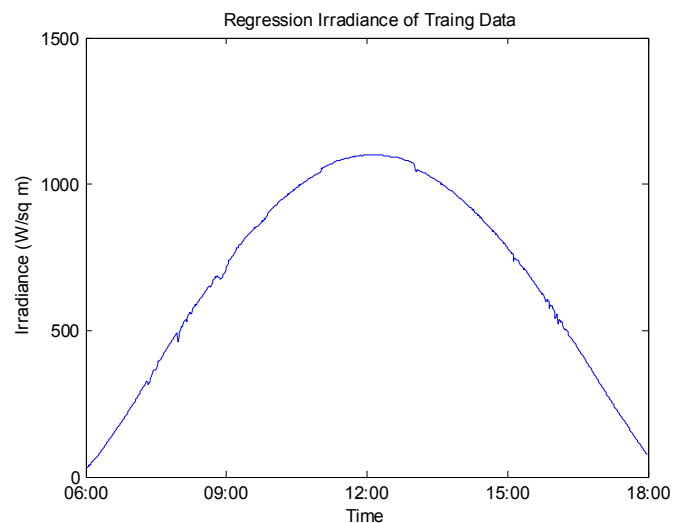
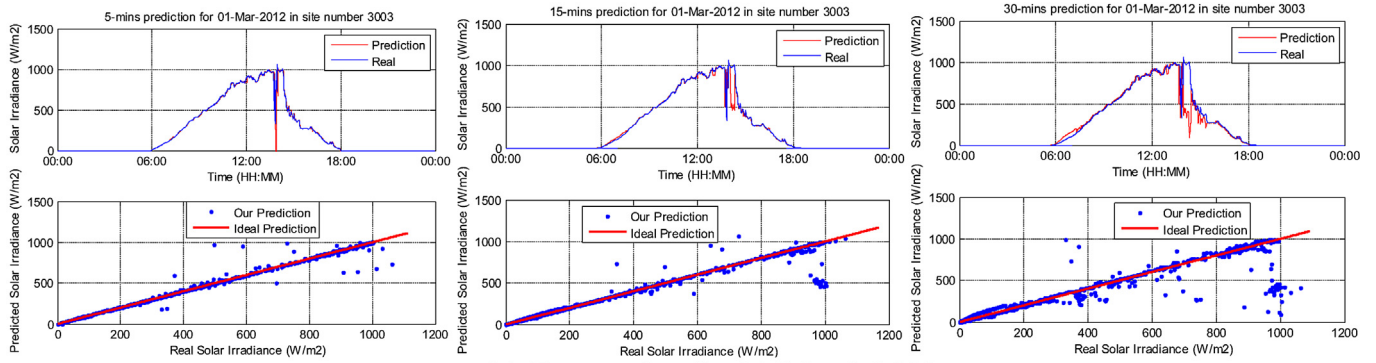
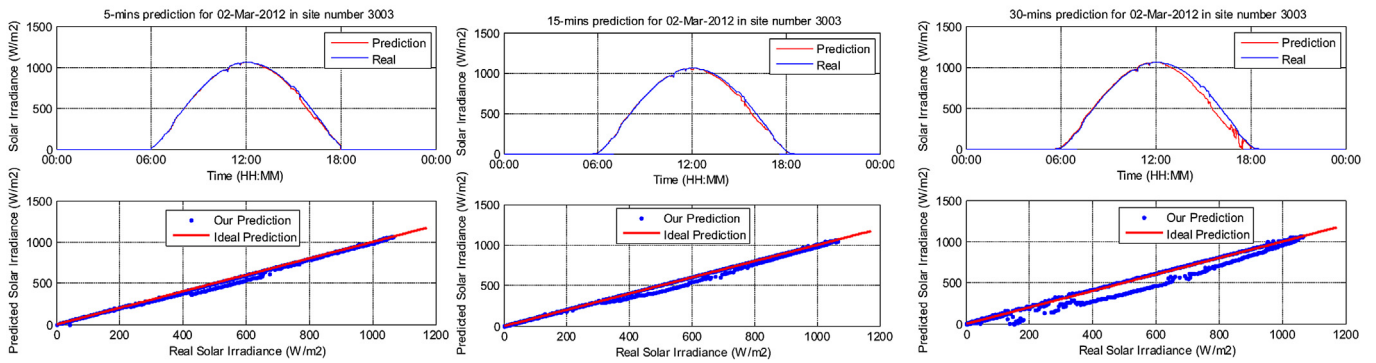


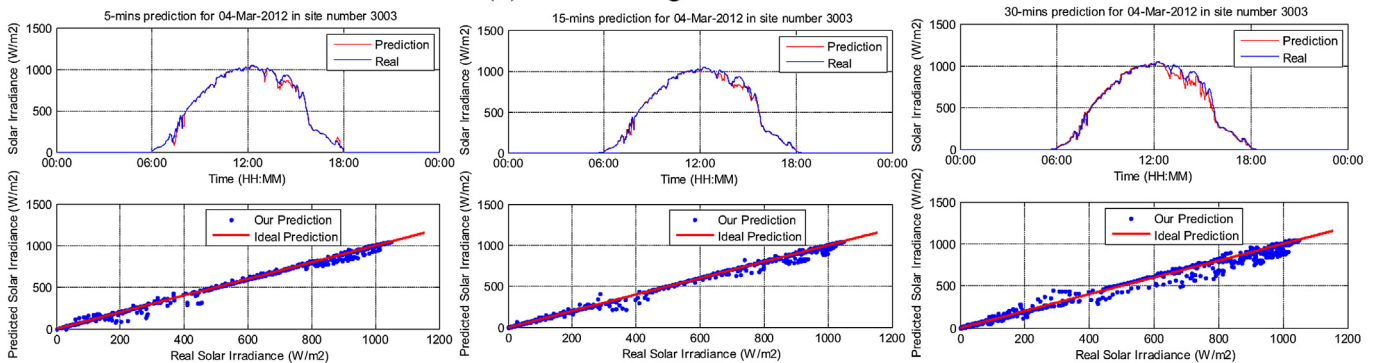
Fig. 9. Regression irradiance of training data.



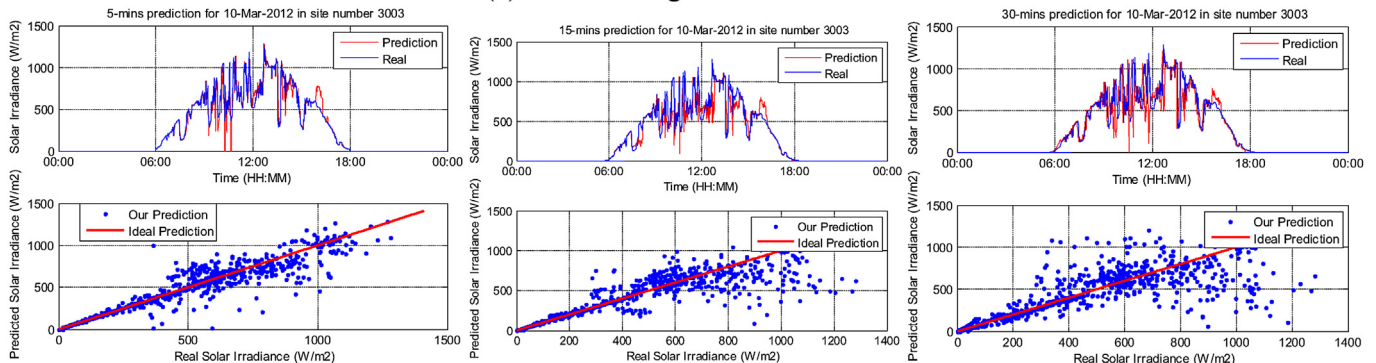
(a) Forecasting for 01-March 2012



(b) Forecasting for 02-March 2012



(c) Forecasting for 04-March 2012



(d) Forecasting for 10-March 2012

Fig. 10. Irradiance forecasting results based on HMM.

$$\begin{aligned} \alpha_i(\varepsilon + \zeta_i - y_i + (w, x_i) + b) &= 0 \\ \alpha_i^*(\varepsilon + \zeta_i^* - y_i + (w, x_i) - b) &= 0 \end{aligned} \quad (10)$$

And

$$\begin{aligned} (C - \alpha_i)\zeta_i &= 0 \\ (C - \alpha_i^*)\zeta_i^* &= 0 \end{aligned} \quad (11)$$

where ζ_i and ζ_i^* are slack variables used to measure errors outside the ε tube. Since $\alpha_i, \alpha_i^* = 0$, and $\zeta_i^* = 0$ for $\alpha_i^* \in (0, C)$, b can be computed as

$$\begin{aligned} b &= y_i - (w, x_i) - \varepsilon, \text{ for } \alpha_i \in (0, C) \\ b &= y_i - (w, x_i) + \varepsilon, \text{ for } \alpha_i^* \in (0, C) \end{aligned} \quad (12)$$

Putting it all together, SVM and SVR can be used without knowing the transformation.

4.2.2. Solar irradiance gradient regression using SVM

SVMs can be applied to regression problems. To collect the data under the same cloud and weather conditions is not easy due to variability between days. As such, we choose sunny and no cloud days as our training data as shown in Fig. 8. Then, an irradiance regression is carried out using SVM. The result is shown in Fig. 9. This regressed irradiance will be saved in the library for calculating irradiance gradients.

4.2.3. Solar irradiance forecasting based on regressed irradiance gradient

Since gradient at time t , δ_t , can be calculated by future and current irradiance as Eq. (13), then based on the regressed irradiance shown in Fig. 9, gradient at any time t can be generated by Eq. (13). In prediction process, this generated gradient of certain time interval can be applied to get predicted irradiance by Eq. (14).

$$\delta_t = \frac{r_{t+N} - r_t}{N} \quad (13)$$

where δ_t is gradient at time t , r_t and r_{t+N} are regressed irradiance values at time t and $t + N$ respectively.

$$\chi_{t+N} = \delta_t \times N + i_t \quad (14)$$

where χ_{t+N} is the forecast irradiance at time $t + N$; i_t is current irradiance values at time t and δ_t is gradient at time t based on regressed solar irradiance.

5. Experimental results

To investigate the accuracy of two solar irradiance forecasting algorithms, a series of simulation experiments were run. All experiments are run under the same platform and test datasets. In this section we report the experimental results.

Data of site number 3003 (Western Australia) from the BOM is selected for testing our irradiance forecasting algorithms. The data in Feb 2012 is used for training and data in March 2012 is used for testing. In order to see how the forecasting algorithms work under

different weather conditions, the data in four different days are selected for comparison, i.e., data on 1st, 2nd, 4th and 10th of March 2012. The data on 1st March has large irradiance changes, related to a sudden weather change; the data on 2nd March is very smooth, which is a sunny day; the data on 4th March varies throughout the day, as it is a cloudy day; and the data on 10th March has very unstable irradiance, as it is a raining day.

5.1. Forecasting based on HMM

The prediction step used in the algorithm can be varied for different time, e.g. 5–30 min. To verify the developed prediction model, the predicted results from the model must be compared with the performance of an actual solar irradiance. Firstly, training data for each day is cut into 8 periods. For each period the range of irradiance variation is generated and also HMM model is trained. These 8 HMM models and ranges of irradiance variations are used for irradiance forecasting in 8 time intervals.

Fig. 10 shows the forecasting results for future N minutes, e.g. 5, 15, 30 min, on the date of 1st, 2nd, 4th and 10th March, 2012. The future N minutes forecasting means the algorithm forecasts what the irradiance will be N minutes from now. Table 1 gives forecasting performance under different weather conditions. From the figure and table we can see that for sunny and cloudy HMM based forecasting has no big performance differences, for very unstable irradiance (raining) day its performance is dropping down. We also see that the forecasting results are promising, especially for 5 min forecasting, for which more than 93% forecasts (sunny and cloudy days) and 65% forecasts (raining days) have prediction accuracy larger than 90%. However, a significant forecasting error comes from irradiance large changes due to clouds. For example at approximately 14:00 on 1st March 2012, there is a massive drop off in the irradiance prediction with no corresponding drop off in the actual irradiance. This is because these large changes are an occasional situation due to clouds, the HMM couldn't pick these up efficiently. If cloud information, such as height, thickness and density, is available, the model on the relationship between cloud and irradiance could be built up. Based on this cloud–irradiance model we would know how the cloud affects the irradiance. Therefore more accurate future irradiance could be predicted. Hopefully these irradiance large changes would be picked up.

5.2. Forecasting based on irradiance gradient regression using SVM

Fig. 11 shows the 5, 15 and 30 min forecasting results on four different weather condition days, 1st, 2nd, 4th and 10th March, 2012. Table 2 gives forecasting performance. From the figure and table we can see that for different weather conditions SVM regression based forecasting has different performance. It works best for sunny days with more than 94% forecasts have prediction accuracy larger than 90%, even for 30 min forecasts.

5.3. Comparison summary of HMM and SVM regression forecasting algorithms

In order to clearly compare the forecasting results of HMM and

Table 1
Forecasting with more than 90% accuracy for HMM based method.

Test day	5-min Prediction	15-min Prediction	30-min Prediction
1 st March 2012 (sudden cloudy)	96%	78.2%	64.6%
2 nd March 2012 (sunny)	93.2%	85.7%	61.8%
4 th March 2012 (cloudy)	92.9%	84.2%	66.8%
10 th March 2012 (raining)	65.4167%	47.8029%	36.3515%

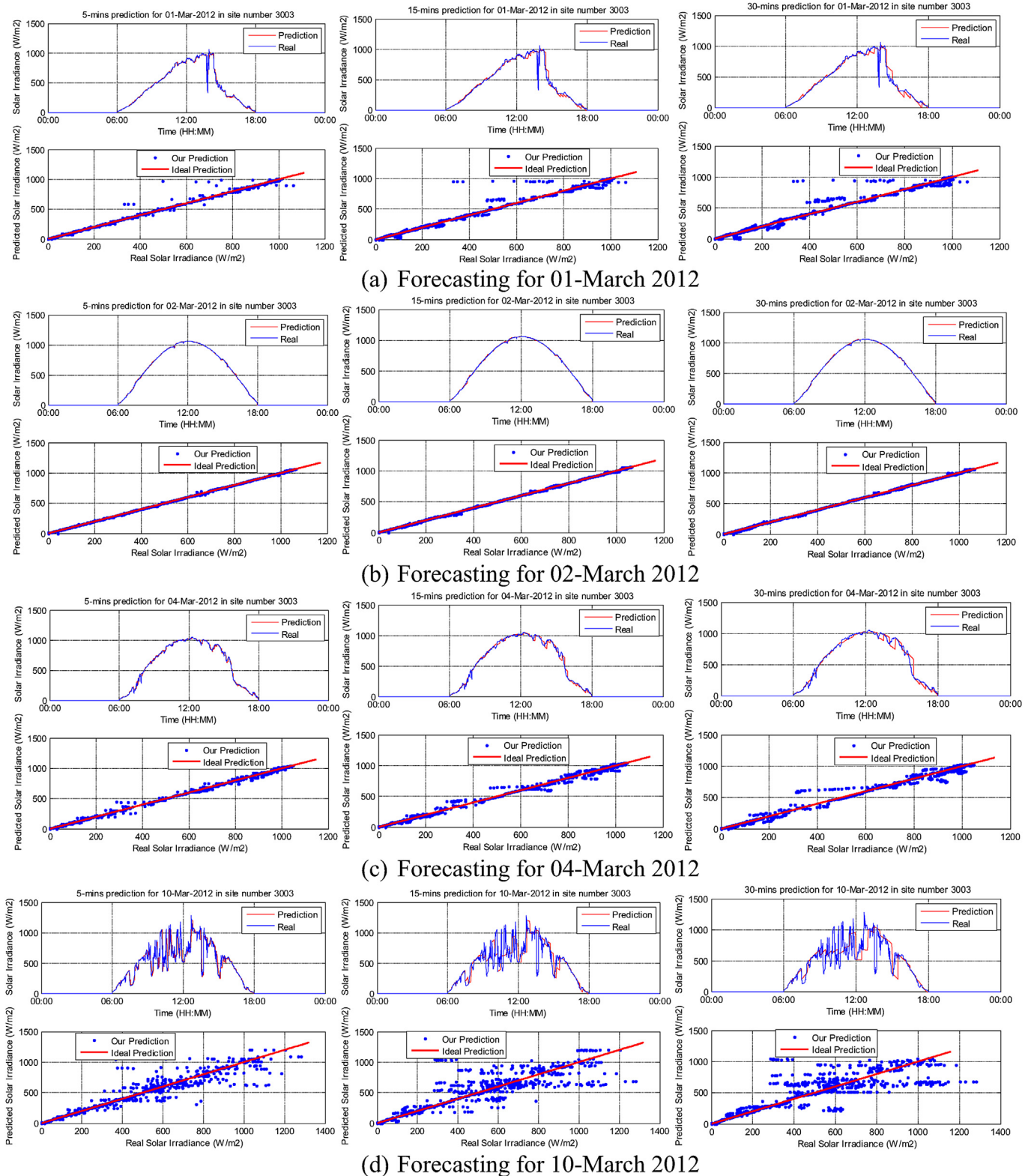


Fig. 11. Irradiance Prediction Results based on Gradient Regression using SVM.

SVM regression algorithms, Table 3 gives same day forecasting performance comparison for 2 methods. Figs. 12–15 show 30-min forecasting results applied to the same day. From the results, we can see that HMM and SVM regression based methods both work well for 5-min forecasting of different weather conditions. For

sunny days, 15-min forecasting SVM regression works better than HMM. For 30-min forecasting, SVM regression works better than HMM for all weather conditions. Overall, for sunny days and long time forecasting, SVM regression works better than HMM. For cloudy days, HMM could better track some small irradiance

Table 2
Forecasting with more than 90% accuracy for SVM regression based method.

Test day	5-min Prediction	15-min Prediction	30-min Prediction
1 st March 2012 (sudden cloudy)	92%	80.4%	73.1%
2 nd March 2012 (sunny)	98.3%	95.6%	94%
4 th March 2012 (cloudy)	92.2%	83.3%	76.3%
20 th March 2012 (raining)	66.9444%	50.4167%	48.4722%

Table 3
Forecasting with more than 90% accuracy for HMM and SVM regression based methods.

Test day	HMM	SVM regression
5-min forecasting		
1 st March 2012 (sudden cloudy)	96%	92%
2 nd March 2012 (sunny)	93.2%	98.3%
4 th March 2012 (cloudy)	92.9%	92.2%
10 th March 2012 (raining)	65.4167%	66.9444%
15-min forecasting		
1 st March 2012 (sudden cloudy)	78.2%	80.4%
2 nd March 2012 (sunny)	85.7%	95.6%
4 th March 2012 (cloudy)	84.2%	83.3%
10 th March 2012 (raining)	47.8029%	50.4167%
30-min forecasting		
1 st March 2012 (sudden cloudy)	64.6%	73.1%
2 nd March 2012 (sunny)	61.8%	94%
4 th March 2012 (cloudy)	66.8%	76.3%
10 th March 2012 (raining)	36.3515%	48.4722%

changes than SVM regression, though needs to be improved for large irradiance changes.

6. Conclusions

HMM and SVM regression based short-term irradiance forecasting algorithms have been investigated and compared under three different weather conditions using the same test platform and datasets. Such forecasting techniques are critical to control solar thermal power levels, schedule fossil fuel powered generators or storage in hybrid renewable mini-grids, reduce fuel costs, increase network stability or maximize system lifetimes. The proposed methods are specifically designed for short-term predictions.

From the results, we can see that two methods work well for sunny days. The performance could be further improved by including irradiance–cloud model in the prediction process by using sky-camera. Data fusion technologies have been widely used to extract useful information from multiple observations and results. These have been applied in various applications such as target tracking, surveillance, robot navigation, signal and image processing [28]. As follow-up work, we will focus on data fusion technology, e.g. Dempster-Shafer [29], to combine these two methodologies to improve the forecasting accuracy under all different weather conditions.

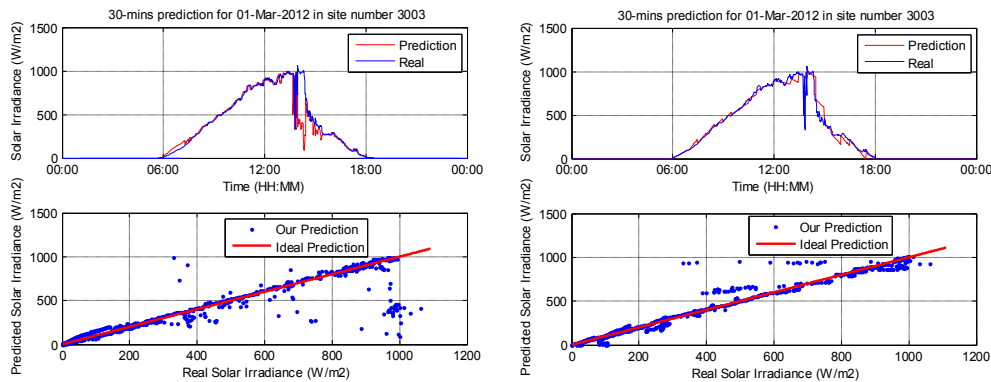


Fig. 12. Irradiance Prediction Results of HMM (left) and SVM regression (right) for 1st March 2012.

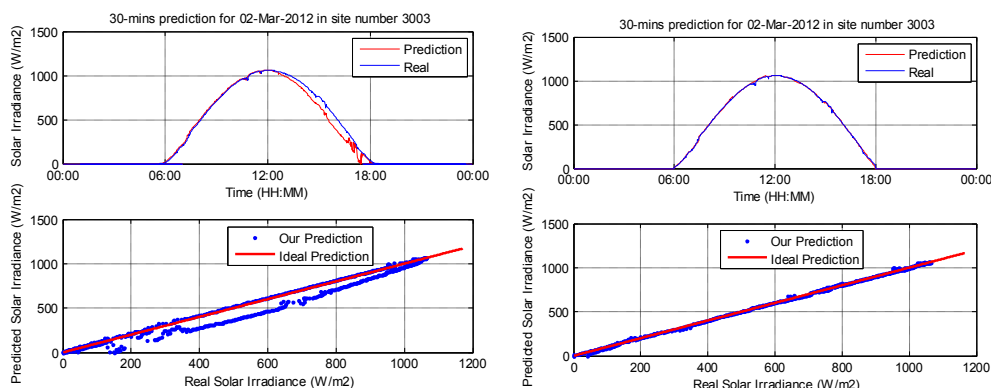


Fig. 13. Irradiance Prediction Results of HMM (left) and SVM regression (right) for 2nd March 2012.

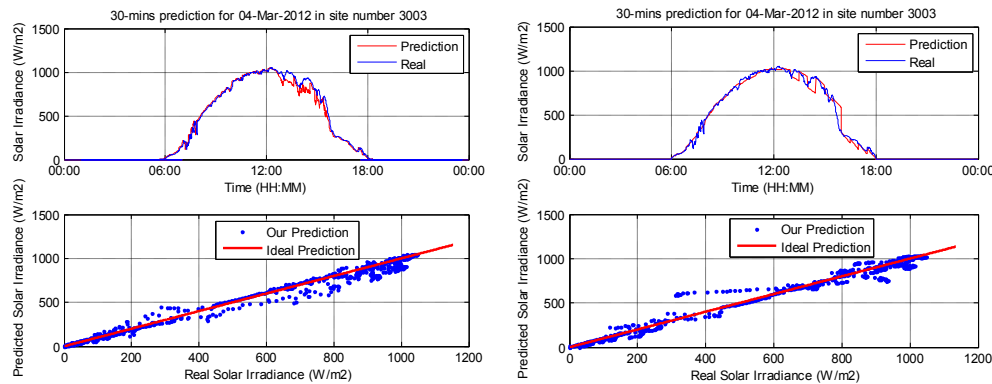


Fig. 14. Irradiance Prediction Results of HMM (left) and SVM regression (right) for 1st March 2012.

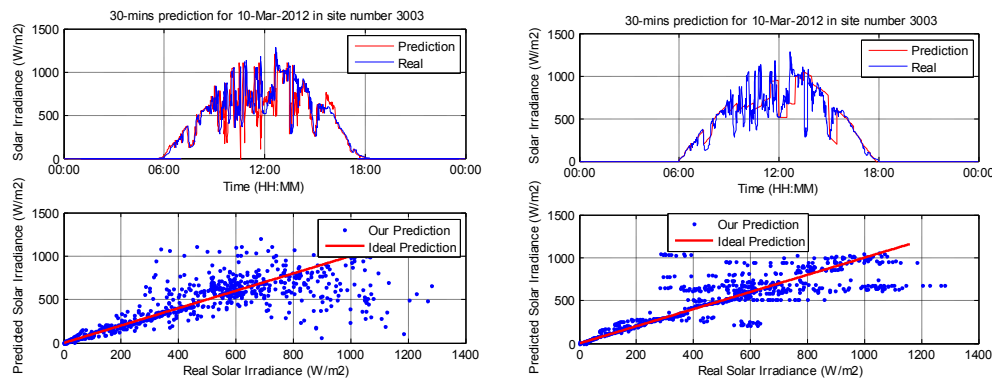


Fig. 15. Irradiance Prediction Results of HMM (left) and SVM regression (right) for 10th March 2012.

Acknowledgment

This project received funding from ARENA, the Australian Renewable Energy Agency (ARENA 2014/RND032). The views expressed herein are not necessarily the views of the Australian Government, and the Australian Government does not accept responsibility for any information or advice contained herein.

References

- [1] C.J. Winter, R.L. Sizman, L.L. Vant-hull, *Solar Power Plants*, Springer-Verlag, USA, 1989.
- [2] G. Platt, Y. Guo, J. Li, S. West, The virtual power station, in: 2008 IEEE International Conference on Sustainable Energy Technologies (ICSET2008) Vols. 1 and 2, Nov. 2008, pp. 526–530.
- [3] J.K. Ward, G. Platt, J. Li, The virtual power station – reliably meeting electricity network demands with photovoltaics, in: 3rd International Solar Energy Society Conference, Sydney, Nov. 2008.
- [4] J. Li, Y. Guo, G. Platt, J.K. Ward, Renewable energy aggregation with intelligent battery controller, *J. Renew. Energy* 59 (November 2013) 220–228.
- [5] M. Diagne, M. David, P. Lauret, J. Boland, N. Schmutz, Review of solar irradiance forecasting methods and a proposition for small-scale insular grids, *Renew. Sustain. Energy Rev.* 27 (2013) 65–76.
- [6] Ajoy, P.K., Popovic, D., *Computational Intelligence in Time Series Forecasting: Theory and Engineering Applications*. Book (Springer).
- [7] Mellit, A., Kalogirou, S.A., Artificial intelligence techniques for photovoltaic applications: a review, *Prog. Energy Combust. Sci.* 34, pp. 547–632.
- [8] K. Chau, A review on integration of artificial intelligence into water quality modeling, *Mar. Pollut. Bull.* 52 (7) (July 2006) 726–733.
- [9] Josh Wall, Jiaming Li, Glenn Platt, An application of a soft real-time genetic algorithm for HVAC system control, *Int. J. Emerg. Trends Technol. Comput. Sci. IJETCS* 2 (3) (2013) 424–434.
- [10] Jiaming Li, Geoff Poulton, Geoff James, Coordination of distributed energy resource agents, *J. Appl. Artif. Intell.* 24 (5) (May 2010) 351–380. <http://www.informaworld.com/smpp/title-db=all-content=t713191765-tab=issueslist-branches=24-v24>.
- [11] Glenn Platt, Jiaming Li, Rongxin Li, Geoff Poulton, Geoff James, Josh Wall, Adaptive HVAC zone modeling for sustainable buildings, *J. Energy Build.* 42 (4) (April 2010) 412–421.
- [12] J.P. Rennard, Introduction to Genetic Algorithms, PhD thesis, 2000.
- [13] H.R. Maier, G.C. Dandy, Neural networks for the prediction and forecasting of water resources variables: a review of modelling issues and applications, *Environ. Model. Softw.* 15 (2000) 101–124.
- [14] J. Faceira, P. Afonso, P. Salgado, Prediction of solar radiation using artificial neural networks, in: Proceedings of the 11th Portuguese Conference on Automatic Control, 321, 2014, pp. 397–406.
- [15] S. Quaiyum, S. Rahman, S. Rahman, Application of artificial neural network in forecasting solar irradiance and sizing of photovoltaic cell for standalone systems in Bangladesh (0975 – 8887), *Int. J. Comput. Appl.* 32 (10) (October 2011).
- [16] A. Mellit, Soteris A. Kalogirou, Mahmoud Drif, Application of Neural Networks and Genetic Algorithms for Sizing of Photovoltaic Systems, Elsevier Journal, 20 May 2010.
- [17] A. Mellit, A.M. Pavan, A 24-h forecast of solar irradiance using artificial neural network: application for performance prediction of a grid-connected pv plant at Trieste, Italy, *Sol. Energy* 84 (5) (2010) 807–821.
- [18] A. Mellit, M. Benghaneim, M. Bendekhis, Artificial neural network model for prediction solar radiation data: application for sizing stand-alone photovoltaic power system, in: Proceedings of IEEE Power Engineering Society, General Meeting, vol. 1, 2005, pp. 40–44.
- [19] Y. Kemmoku, S. Orita, S. Nakagawa, T. Sakakibara, Daily insolation forecasting using a multi-stage neural network, *Sol. Energy* 66 (3) (1999) 193–199.
- [20] A. Sfetos, A.H. Coonick, Univariate and multivariate forecasting of hourly solar radiation with artificial intelligence techniques, *Sol. Energy* 68 (2) (2000) 169–178.
- [21] G. Mihalakakou, M. Santamouris, D.N. Asimakopoulos, The total solar radiation time series simulation in Athens, using neural networks, *Theor. Appl. Climatol.* 66 (3–4) (August 2000) 185–197.
- [22] F.O. Hocaoglu, ÖN. Gerek, M. Kurbani, A novel 2-d model approach for the prediction of hourly solar radiation, in: Computational and Ambient Intelligence, Springer, 2007, pp. 749–756.
- [23] M.N. French, W.F. Krajewski, R.R. Cuykendall, Rainfall forecasting in space and time using a neural network, *J. Hydrology* 137 (1992) 1–31.
- [24] Zoubin Ghahramani, An introduction to hidden Markov models and Bayesian networks, *Int. J. Pattern Recognit. Artif. Intell.*, Vol. 15, No. 1, p. 9–42.
- [25] A.T. Bharucha-Reid, *Elements of the Theory of Markov Processes and Their Applications*, McGraw-Hill, New York, 1960.

- [26] L.R. Rabiner, A tutorial on hidden Markov models and selected applications in speech recognition, Proc. IEEE 77 (1989) 257–286.
- [27] L.R. Rabiner, A tutorial on hidden Markov models and selected applications in speech recognition, Proc. IEEE 77 (2) (1989) 257–286.
- [28] Zou Yi, Yeong Khing Ho, Chin Seng Chua, Xiao Wei Zhou, Multi-ultrasonic sensor fusion for mobile robots, in: Proceedings of the IEEE Intelligent Vehicles Symposium 2000, Dearborn(MI), USA October 3–5, 2000.
- [29] J. Li, S. Luo, J.S. Jin, Sensor data fusion for accurate cloud presence prediction using Dempster-Shafer evidence theory, Sensors 10 (10) (2010) 9384–9396.